

1                   **Topographic control of snowpack**  
2                   **distribution in a small catchment in the**  
3                   **central Spanish Pyrenees: intra- and inter-**  
4                   **annual persistence**

5  
6                   **J.Revuelto<sup>1</sup>, J.I. López-Moreno<sup>1</sup>, C. Azorin-Molina<sup>1</sup>, S.M. Vicente-Serrano<sup>1</sup>**

7  
8                   <sup>1</sup> *Instituto Pirenaico de Ecología, Consejo Superior de Investigaciones Científicas (IPE-*  
9                   *CSIC) Departamento de Procesos Geoambientales y Cambio Global, Campus de Aula Dei,*  
10                   *P.O. Box 13034, 50059, Zaragoza, Spain*

11  
12  
13                   *Email addresses: [jrevuelto@ipe.csic.es](mailto:jrevuelto@ipe.csic.es), [nlopez@ipe.csic.es](mailto:nlopez@ipe.csic.es), [cazorin@ipe.csic.es](mailto:cazorin@ipe.csic.es),*  
14                   *[svicen@ipe.csic.es](mailto:svicen@ipe.csic.es)*

15  
16  
17                   \* Corresponding author: [jrevuelto@ipe.csic.es](mailto:jrevuelto@ipe.csic.es)

22 **Abstract:**

23 In this study we analyzed the relations between terrain characteristics and snow depth  
24 distribution in a small alpine catchment located in the central Spanish Pyrenees. Twelve field  
25 campaigns were conducted during 2012 and 2013, which were years characterized by very  
26 different climatic conditions. Snow depth was measured using a long range terrestrial laser  
27 scanner and analyses were performed at a spatial resolution of 5 m. Pearson's  $r$  correlation,  
28 multiple linear regressions and binary regression trees were used to analyze the influence of  
29 topography on the snow depth distribution. The analyses were used to identify the  
30 topographic variables that best explain the snow distribution in this catchment, and to assess  
31 whether their contributions were variable over intra- and inter-annual time scales. The  
32 topographic position index (index that compares the relative elevation of each cell in a digital  
33 elevation model to the mean elevation of a specified neighborhood around that cell with a  
34 specific shape and searching distance), which has rarely been used in these types of studies,  
35 most accurately explained the distribution of snow accumulation. Other variables affecting the  
36 snow depth distribution included the maximum upwind slope, elevation, and northing. The  
37 models developed to predict snow distribution in the basin for each of the 12 survey days  
38 were similar in terms of the explanatory variables. However, the variance explained by the  
39 overall model and by each topographic variable, especially those making a lesser contribution,  
40 differed markedly between a year in which snow was abundant (2013) and a year when snow  
41 was scarce (2012), and also differed between surveys in which snow accumulation or melting  
42 conditions dominated in the preceding days. The total variance explained by the models  
43 clearly decreased for those days on which the snow pack was thinner and more patchily.  
44 Despite the differences in climatic conditions in the 2012 and 2013 snow seasons, similarities  
45 in snow distributions patterns were observed which are directly related with terrain  
46 topographic characteristics.

47 **Keywords:** snow depth distribution, snowpack evolution, topography, mountains, cold region

## 48 **1. Introduction**

49 Assessing the snow distribution in mountain areas is important because of the number of  
50 processes in which snow plays a major role, including erosion rates (Pomeroy and Gray,  
51 1995), plant survival (Keller et al., 2000; Wipf et al., 2009), soil temperature and moisture  
52 (Groffman et al., 2001), and the hydrological response of mountain rivers (Bales and  
53 Harrington, 1995; Barnett et al., 2005; Liston, 1999; Pomeroy et al., 2004). As mountain areas  
54 are highly sensitivity to global change (Beniston, 2003), snow accumulation and melting  
55 processes are likely to be subject to marked changes in coming decades, affecting all  
56 processes influenced by the presence of snow (Caballero et al., 2007; López-Moreno et al.,  
57 2011, 2012b; Steger et al., 2012). For these reasons, much effort has been devoted to  
58 understanding the main factors that control the spatial and temporal dynamics of snow (Egli et  
59 al., 2012; López-Moreno et al., 2010;; Mott et al., 2010; Schirmer et al., 2011).

60 One of the main difficulties in snow studies is obtaining reliable information of the variables  
61 that describe snow distribution, including snow depth (SD), snow water equivalent (SWE)  
62 and snow covered area (SCA). Manual measurements have traditionally been used to provide  
63 information on the distribution of snowpack, with different sampling strategies having been  
64 applied at various spatial scales (Jost et al., 2007; López-Moreno et al., 2012a; Watson et al.,  
65 2006). However, manual sampling is not feasible for large areas because of the time involved,  
66 especially when SWE measurements are also acquired. In the last decade the use of airborne  
67 laser scanners (ALS) (Deems et al., 2006) and terrestrial laser scanners (TLS) (Prokop, 2008),  
68 both of which are based on LiDAR (light detection and ranging) technology, have provided  
69 for major advances in obtaining data on the SD distribution at unprecedented spatial  
70 resolutions. These developments have enabled studies of several factors that in the past have  
71 been only marginally considered, including scaling issues (Fassnacht and Deems, 2006; Mott  
72 et al., 2011; Schirmer and Lehning, 2011; Trujillo et al., 2007), the detailed dynamics of snow  
73 accumulation and ablation (Grünewald et al., 2010; Schirmer et al., 2011; Scipión et al.,

74 2013), and snow transport processes (Mott et al., 2010). In addition, the high density  
75 measurements provided by LiDAR technologies are a valuable resource for detailed  
76 investigation of the linkage between snow distribution and topography. In the past, this  
77 linkage has mostly been studied using manual measurements, and hence with generally  
78 limited spatial and temporal resolution (López-Moreno et al., 2010).

79 Previous studies have highlighted the marked control of topography on snow distribution in  
80 mountain areas (Anderton et al., 2004; Erickson et al., 2005; Lehning et al., 2011; Mott et al.,  
81 2013), and the importance of vegetation and wind exposure (Erxleben et al., 2002; Trujillo et  
82 al., 2007). The most commonly used approach has been to develop digital elevation models  
83 (DEM) that describe the spatial distribution of elevation, from which other terrain variables  
84 are derived such as slope, terrain aspect, curvature, wind exposure or sheltering, and potential  
85 solar radiation. This enables to analyze the linear or non-linear relation of these variables to  
86 punctual SD or SWE values to be established (Grünwald et al., 2010; Schirmer et al., 2011).  
87 Various statistical methods have been applied for this purpose, including linear regression  
88 models (Fassnacht et al., 2003; Hosang and Dettwiler, 1991), generalized additive models  
89 (GAM) (López-Moreno and Nogués-Bravo, 2005), and binary regression trees (BRT)  
90 (Breiman, 1984) which have been widely applied in a diversity of regions (Elder et al., 1991;  
91 Erxleben et al., 2002; McCreight et al., 2012;)

92 The extent to which topographic variables explain snow distribution can change during the  
93 snow season; the variability of terrain characteristics can drive processes related to the spatial  
94 variability of snow accumulation (snow blowing, terrain curvature) (Lehning et al., 2008), or  
95 affect the energetic exchange between terrain and the snowpack (temperature, incoming solar  
96 radiation), so the importance of topographic variables is modified during the season (Molotch  
97 et al., 2005). In addition, during a snow season the terrain changes markedly (is smoothed) by  
98 snow accumulation (Schirmer et al., 2011). However, few studies have systematically  
99 analyzed the intra- and inter-annual persistence of the relation between snow distribution and

100 topography. Recent studies have assessed whether the influence of topography is constant  
101 among different years; e.g. the similarities observed at the end of the accumulation season  
102 (Schirmer and Lehning, 2011; Schirmer et al., 2011), or the consistent fractal dimensions in  
103 two analyzed years (Deems et al., 2008); in both cases there was a relation with the dominant  
104 wind direction, which highlights the predictive ability of topographic variables.

105 The main focus of this study was to assess the influence of topography on the spatial  
106 distribution of snowpack and its evolution over time. The high temporal and spatial density of  
107 the dataset collected during the study enabled analysis of the main topographic factors  
108 controlling snow distribution, and assessment of whether topographic control of the snowpack  
109 varied during the snow season and between years having very contrasting climatic conditions.  
110 For this purpose, we conducted 12 surveys over 2012 (6) and 2013 (6) in a small mountain  
111 catchment representing a typical subalpine environment in the central Spanish Pyrenees, and  
112 obtained high resolution SD measurements using LIDAR technology using a TLS.

## 113 **2. Study area and snow and climatic conditions**

114 The Izas experimental catchment (42°44'N, 0°25'W) is located in the central Spanish  
115 Pyrenees (Fig. 1). The catchment is on the southern side of the Pyrenees, close to the main  
116 divide (Spain–France border), in the headwaters of the Gallego River valley, and ranges in  
117 elevation from 2000 to 2300 m above sea level. The catchment is predominantly east-facing,  
118 with some areas facing north or south, and has a mean slope of 16°. There are no trees in the  
119 study area, and the basin is mostly covered by subalpine grasslands dominated by *Festuca*  
120 *eskia* and *Nardus stricta*, with rocky outcrops in the steeper areas; flat, concave and convex  
121 areas occur in the basin.

122 The climatic conditions are influenced by the proximity of the Atlantic Ocean, with the  
123 winters being humid compared with zones of the Pyrenees more influenced by mediterranean  
124 conditions. The mean annual precipitation is 2000mm, of which snow accounts for

125 approximately 50% (Anderton et al., 2004). The mean annual air temperature is 3°C, and the  
126 mean daily temperature is < 0°C for an average of 130 days each year (del Barrio et al.,  
127 1997). Snow covers a high percentage of the catchment from November to the end of May  
128 The two years analyzed in the study represent climatic extremes during recent decades.  
129 Severe drought occurred during 2012, leading to snow accumulation well below the long-term  
130 average. The thickness of the snowpack, measured at the automatic weather station (AWS,  
131 Fig. 1), during winter in this year was less than the 25th percentile of the available historical  
132 data series of this AWS (1996–2011) (Fig. 2). Only at the end of spring did late snowfall  
133 events increase the amount of snow, but this rapidly melted. The opposite occurred in 2013,  
134 which was a year in which the deepest snowpack and the longest snow season of recent  
135 decades were recorded. Winter and spring in 2013 were extremely humid, with temperatures  
136 mostly between the 25th and 75th percentiles of the AWS historical series. Snow depth  
137 accumulation was very high between February and June (exceeding the 75th percentile); in  
138 some areas of the basin it lasted until late July, which is one month longer than in most of the  
139 preceding years for which records are available.

### 140 **3. Data and methods**

#### 141 **3.1. Snow depth measurements**

142 During the study period high resolution SD maps were generated using a long range TLS  
143 (Riegl LPM-321), which enables safe acquisition of SD information with short acquisition  
144 times from remote areas, compared with measurements obtained manually. This technique  
145 has been extensively tested (Prokop et al., 2008; Revuelto et al., 2014; Schaffhauser et al.,  
146 2008), and systematically applied to the study of snow distribution in mountain terrain (Egli  
147 et al., 2012; Grünewald et al., 2010; Mott et al., 2013; Schirmer et al., 2011). In a previous  
148 study the mean absolute error in the most distant areas of the catchment was less than 10cm

149 (Revuelto et al., 2014), which is consistent with errors reported in previous studies  
150 (Grünewald et al., 2010; Prokop, 2008; Prockop et al., 2008; Schaffauser et al., 2008).

151 TLS provides high resolution three dimensional information on the terrain Nevertheless, error  
152 sources need to be considered because they can have large effects on the measurements. To  
153 reduce the influences of TLS instability (originated by small displacements of the tripod  
154 because TLS vibrations while it is operating), which leads to misalignment with reference  
155 points; and atmospheric change, a well-defined protocol must be applied. The protocol  
156 applied in this study for generating high resolution SD maps with a 1m cell size was described  
157 by Revuelto et al., (2014). This protocol has these main points: data collection; which  
158 includes experimental setup design and information acquisition by the scanning procedure;  
159 and data processing, where data is filtered, quality checked and the SD maps generated.  
160 Mainly, the methodology was based on differences between DEMs obtained with snow  
161 coverage in the study area and a DEM taken at 18 July 2012, when the catchment had no  
162 snow cover. Twelve snow depth maps at a spatial resolution of 5m were generated for the  
163 2012 and 2013 snow seasons (Fig. 3). In each year three surveys were undertaken from  
164 February to April (2012: 22 February, 2 April, 17 April; 2013: 17 February, 3 April, 25  
165 April), and three were undertaken from May to June when dominated intense melting  
166 conditions (2012: 2, 14 and 24 May; 2013: 6, 12 and 20 June). The average SD and SCA, and  
167 the maximum SD are shown in Table 1. It shows that much lower SD and SCA were observed  
168 in 2012 compared to 2013.

### 169 **3.2. Digital elevation model and topographic variables**

170 From the two scan stations located in the study area (Fig. 1), 86% of the total area of the  
171 catchment was surveyed using TLS. DEMs of 1m grid size were initially obtained from point  
172 clouds of varying density in different areas, but always with a minimum of 1point/m<sup>2</sup>  
173 (Revuelto et al., 2014). Some of the predictor variables cannot be calculated where data gaps  
174 occur in the DEM (e.g. the topographic position index), and others require a DEM with a

175 greater surface than the area scanned during the study (e.g. to calculate the potential solar  
176 radiation, including the shadow effect from surrounding topography, or to calculate the  
177 maximum upwind slope parameter, it is included topographic information for distances up to  
178 1200m from the exterior limit of the DEM obtained with the TLS). Thus, a DEM having a 5  
179 m grid-size, available from the Geographical National Institute of Spain (Instituto Geográfico  
180 Nacional, [www.ign.es](http://www.ign.es)), was combined with the snow-free DEM obtained using the TLS  
181 resampled from 1 m to 5 m resolution (the empty raster of the Geographical National Institute  
182 was used for the resampling, averaging all values within each cell). The 1 m grid-size SD  
183 maps were also resampled to 5 m to enable matching of the two different data sources.

184 To characterize the terrain characteristics, eight variables were derived from the final DEM,  
185 including: (i) elevation (*Elevation*), (ii) slope (*Slope*), (iii) curvature (*Curvature*), (iv)  
186 potential incoming solar radiation under clear sky conditions (*Radiation*), (v) easting exposure  
187 (*Easting*), (vi) northing exposure (*Northing*), (vii) the topographic position index (*TPI*) and  
188 (viii) maximum upwind slope (*Sx*).

189 *Elevation* was obtained directly from the DEM, while the other variables were calculated  
190 using ArcGIS10.1 software. This calculates *Slope* as the maximum rate of change in value  
191 from a specific cell to that of its neighbors (10 m window size), and *Curvature* is determined  
192 from the second derivative of the fitted surface to the DEM in the direction of maximum slope  
193 of the terrain for the neighbors cells (10 m window size too). *Radiation* was obtained using  
194 the algorithm of Fu and Rich (2002) and reported in Wh/m<sup>2</sup> meter based on the average  
195 conditions for the 15-day period prior to each snow survey. This algorithm calculates the  
196 potential clear sky radiation, which logically may strongly differ from the real radiation as a  
197 consequence of cloud cover. This measure provided the relative difference in the  
198 extraterrestrial incoming solar radiation among areas of the catchment for a given period  
199 under given topographical conditions (Fassnacht et al., 2013). *Easting* and *Northing* exposure  
200 were calculated directly as the sine and cosine, respectively, of the angle between direction

201 north and terrain orientation or aspect. It provided information on the east (positive)/west  
202 (negative) exposure and the north (positive)/south (negative) exposure.

203 The *TPI* provides information on the relative position of a cell in relation to the surrounding  
204 terrain at a specific spatial scale. Thus, this index compares the elevation of each cell with the  
205 average cell elevation at specific radial distances as follows (De Reu et al., 2013; Weiss,  
206 2001):

$$207 \quad TPI = z_o - \bar{z} \quad (1)$$

$$208 \quad \bar{z} = \frac{1}{n_R} \sum_{i \in R} z_i \quad (2)$$

209 Where  $z_o$  is the elevation of the cell in which *TPI* is calculated and  $\bar{z}$  is the average elevation  
210 of surrounding cells obtained from (2) for a radial distance  $R$ . For each pixel the *TPI* was  
211 calculated for 5, 10, 15, 25, 50, 75, 100, 125, 150 and 200 meters radial distances (scale  
212 factors).

213 For specific wind directions, the maximum upwind slope parameter, averaged for 45° upwind  
214 windows (*Sx dash*; Winstral et al., 2002) provided information on the exposure or sheltering  
215 of individual cells at various distances, resulting from the topography. Rather than  
216 considering the contribution for the dominant wind directions (Molotch et al., 2005), *Sx dash*  
217 (*Sx* further on) values for eight directions were selected and directly related to the SD. The  
218 directions were: 0° for north (N), 45° for northeast (NE), 90° for east (E), 135° for southeast  
219 (SE), 180° for south (S), 225° for southwest (SW), 270° for west (W), and 315° for northwest  
220 (NW). For *Sx* the searching distances (Winstral et al., 2002) considered were 100, 200, 300  
221 and 500m. These distances were selected to enable assessment of the range at which *Sx*  
222 exhibited greatest control on SD dynamics, as has occurred in previous studies (Schirmer et  
223 al., 2011; Winstral et al., 2002).

### 224 **3.3. Statistical analysis**

225 The 12 SD maps at 5 m spatial resolution were related to each of the topographic variables  
226 considered (including the 40 *Sx* combinations, and the 9 distances for *TPI*). The large number  
227 of cells for which snow depth data were available enabled robust correlations between  
228 topography and snow distribution to be obtained, and provided a very large dataset for  
229 training and validation of the SD distribution models.

230 Pearson's *r* coefficients were obtained between SD and each topographic variable. Using the  
231 whole dataset each variable was correlated, for all available points, against the SD value for  
232 the specific survey day. Given the large amount of data for surveys, the degrees of freedom  
233 for the correlation analyses were very high and hence it can inform of statistically significant  
234 correlations even with very low correlation coefficients. Moreover, the use of a very dense  
235 dataset of observations may have associated problems derived from spatial autocorrelation  
236 (Elsner and Schmertmann, 1994). For this reason we followed a Monte Carlo procedure, in  
237 which 1000 random samples of 100 SD cases were extracted from the entire dataset and  
238 correlated with topographic variables for assessing significance. A threshold 95% confidence  
239 interval ( $\alpha < 0.05$ ) was used to assess the significance of correlations ( $r = \pm 0.197$ , based on  
240 100 cases). The spatial scales of *Sx* and *TPI* for which SD showed a higher correlation; 200m  
241 and 25m respectively, were selected for further analysis (not presented in the manuscript).

242 To assess the explanatory capacity when all topographic variables were considered  
243 simultaneously, two statistical models were used: (1) multiple linear regressions (MLRs) and  
244 (2) binary regression trees (BRTs). A wide variety of regression analyses for interpretation of  
245 much more complex spatial data are available with greater capacity than MLRs and BRTs to  
246 deal with spatial autocorrelation issues and the non-linear nature of the relationship between  
247 predictors and the response variable (Beale et al., 2010). However, in this study we used  
248 MLRs and BRTs because these methods have been and are still widely used in snow studies,  
249 and because both enable to isolate accurately the weight of each independent variable within  
250 the model, which was the main objective of this research, rather than deriving models with

251 maximum predictive capacity. Prior to run the models a principal component analysis (PCA)  
252 was applied to the topographic variables for detecting correlations between independent  
253 variables that could originate multicollinearity in MLR and BRT. This analysis (not shown)  
254 grouped the topographic variables in three components, from which it is observed that *TPI*  
255 and *Curvature* are highly correlated, and also *Northing* and *Radiation* (but in this case  
256 inversely) presented almost identical correlations with the three identified components. As  
257 *TPI* and *Northing* showed higher correlations with their respective components and also show  
258 in general higher Pearson's r coefficients with SD (see result section), the variables *Curvature*  
259 and *Radiation* were discarded as predictors in MLR and BRT analyses.

260 (1) *Multiple linear regression* estimates the linear influence of topographic variables on SD.

261 Despite its simplicity and the rather limited capability under nonlinear conditions (López-  
262 Moreno et al., 2010), MLR was used to quantify the relative contribution of each variable  
263 to the entire SD distribution model. SD was calculated from the topographic variables at  
264 a specific location for a given day. The threshold for a variable to enter in the model was  
265 set at  $\alpha < 0.05$ . Beta coefficients (obtained dividing the standardized units by the  
266 coefficients by the mean value of each variable) were used to compare the weight of each  
267 variable within the regression models. Again, in order to avoid an excessive number of  
268 observations that may lead to spurious identification of statistically significant predictor  
269 variables, we first randomly extracted a reduced dataset (1000 cases) for selecting the  
270 topographic variables by means of a stepwise procedure. Once variables to be included  
271 for each survey were determined, they were used to obtain the final model, but using the  
272 entire data set (except 5000 cases for model validation), forcing variables entrance in  
273 models.

274 (2) *Binary regression trees* have been widely used to model snowpack distribution from  
275 topographic data (Erxleben et al., 2002; Molotch et al., 2005). These are nonparametric  
276 models that recursively split the data sample, based on the predictor variable that

277 minimizes the square of the residuals obtained (Breiman, 1984). One BRT was created  
278 for each sampling date. The BRTs were run until a new split was not able to account for  
279 1% of the explained variance, or when a node had less than 500 cases; a maximum of 15  
280 terminal nodes was set, to reduce tree complexity. As there were no over-fitting problems  
281 associated with sample size, 15,000 cases were used to grow the trees and 5,000 cases  
282 were used for validation. By scaling the explained variance of each variable introduced  
283 into each BRT (based on the % of the total explained variance by the BRT), we were able  
284 to compare the relative importance of each topographic variable between the different  
285 models.

286 Coefficients of determination ( $r^2$ ) and Willmott's D statistic were used to assess the ability of  
287 each model to predict snow depth over an independent random sample of 5,000 cases.

288 Willmott's D was determined using equation (3) (Willmott, 1981):

$$289 \quad D = 1 - \frac{\sum_{i=1}^N (P_i - O_i)}{\sum_{i=1}^N (|P_i - \bar{O}| + |O_i - \bar{O}|)^2} \quad (3)$$

290 where N is the number of observations,  $O_i$  is the observed value,  $P_i$  is the predicted value, and  
291  $\bar{O}$  is the mean of the observed values. The index ranges from 0 (minimum) to 1 (maximum  
292 predictive ability).

## 293 **4. Results**

### 294 **4.1. Single correlations**

295 Table 2 shows the correlation between SD and  $S_x$  for the eight wind directions at a distance of  
296 200 m (identified as the best correlated searching distance in previous analysis). Despite  
297 differences in magnitude, the correlations for surveys carried out at the beginning of the  
298 season (22 February 2012 and 17 February 2013) in each year showed that SD was clearly  
299 affected by N and NW wind directions. This was particularly evident in 2013, as the  
300 correlation values were higher for both days. The contribution of N and NW wind directions  
301 is clearly evident for the surveys on 17 February 2013 (Figure 4, were wind roses with

302 average wind speeds and direction, for the 15 day period before each survey are presented),  
303 when greater SD was recorded in the leeward slopes from a northerly direction (Fig. 3, upper  
304 areas of the maps). In the two years of the study a correlation with W and SW wind directions  
305 was observed to increase progressively during the snow season (Fig. 4 and Table 2  
306 correlations). In 2013 this phenomenon was less marked because of the greater SD  
307 accumulation at the beginning of the snow season accompanied with NW direction winds,  
308 which resulted in only moderate changes in the  $S_x$  for the most strongly correlated wind  
309 directions. It was also observed that in both study years once the snow had started to melt (the  
310 last three surveys in each season) the snow distribution did not change in relation to  $S_x$   
311 directions. When the best correlated  $S_x$  directions for each survey are compared with wind  
312 roses (Fig. 4) a good agreement is observed. These directions for survey days are:  $315^\circ$  for 22  
313 Feb. 2012,  $270^\circ$  for 02 and 17 April 2012, and  $225^\circ$  for the three surveys in May 2012; in  
314 2013,  $315^\circ$  was the best correlated direction for 17 Feb. and  $270^\circ$  for the other five surveys of  
315 the snow season

316 Correlations between the most correlated  $S_x$  direction for each day and SD were compared  
317 with correlations between SD and the other topographic variables (Table 3). This showed that  
318  $S_x$  had one of the greatest coefficient of correlation with SD (range 0.22–0.56). The  
319 correlations were higher during the accumulation periods, especially in the 2013 snow season,  
320 with a reduction in correlations values occurring during the melt period at the end of each  
321 snow season.

322 The  $TPI$  at 25 m showed the highest correlation with SD for nearly all of the 12 sampled days.  
323 During 2012 the mean correlation values ranged from  $-0.32$  to  $-0.58$  for those surveys during  
324 which snow accumulation dominated in the days preceding the surveys. The  $r$  values were  
325 closer to the significance level for the surveys where the preceding days were dominated by  
326 melting conditions (14 and 24 May). In 2013, the  $TPI$  was more highly correlated with SD  
327 than in 2012, with Pearson's  $r$  coefficients  $< -0.6$  for all survey days. *Curvature* also had a

328 high correlation with SD, and similar to *TPI* with a 25 m searching distance was significantly  
329 correlated on all the survey dates, but unlike the *TPI*, the correlation of *Curvature* with SD did  
330 not decrease during the snowmelt periods. The significant correlations of *TPI* and *Curvature*  
331 with SD highlight the importance of terrain curvature on the SD distribution. The importance  
332 of terrain curvature at different scales for SD distribution is clearly evident in Figure 3, which  
333 shows that higher SD values were usually found for concave areas, which showed snow  
334 presence until the end of each snow season.

335 The correlation between *Elevation* and SD varied among survey days (Table 3). The  
336 correlations were usually positive, but only statistically significant (or approaching  
337 significance) for days when melting dominated (the last two surveys in 2012 and 2013). *Slope*  
338 was relatively weakly correlated with SD during the 2012 snow season. In 2013 the  
339 correlation was greater, and was statistically significant on some days. As with *Elevation*, the  
340 correlation between *Slope* and SD was variable between the two study years, and showed a  
341 similar temporal pattern to *Easting*, probably because of the presence of steeper areas on the  
342 east-facing slopes.

343 The correlation between *Northing* and SD was rarely statistically significant, was highly  
344 variable, and contributed to explaining SD in a very different ways in 2012 and 2013. In 2012  
345 no correlation between SD and *Northing* was found during the accumulation period, but  
346 during the melting period a slight positive correlation was observed, as snow remained longer  
347 on north-facing slopes. The 2013 snow season started with a large precipitation event  
348 dominated by strong winds from a northerly direction, leading to high levels of snow  
349 accumulation on the south-facing slopes. This explains the strong and statistically significant  
350 negative correlation of SD with *Northing* for 17 February 2013. This event influenced the rest  
351 of the season (as evident in Table 2 in 2013), but a progressive decrease in its influence was  
352 evident for the following survey days. *Radiation* had an almost opposite influence on SD to  
353 that observed for *Northing*. During the melting period in each year the Pearson's  $r$  correlation

354 between SD and *Radiation* was negative, indicating a thinner snowpack on the most irradiated  
355 slopes; the relation was statistically significant at the end of the 2013 snow season. However,  
356 during the accumulation period in 2013 statistically significant positive correlations were  
357 observed with *Northing* and *Radiation*, which are connected to the strong snow redistribution  
358 by winds from N-NW directions.

#### 359 **4.2. Multiple Linear Regression and Binary Regression Tree models**

360 Figure 5 shows the Willmott's D values and the coefficients of determination ( $r^2$ ) obtained in  
361 the comparison of observed and predicted values using MLRs and BRTs for a dataset  
362 reserved for validation (5000 cases). The MLRs produced  $r^2$  values ranging from 0.25 to 0.65  
363 and Willmott's D values ranging from 0.60 to 0.88, while the BRTs produced  $r^2$  values  
364 ranging from 0.39 to 0.58 and Willmott's D values ranging from 0.72 and 0.85. For both  
365 methods the relationship between the observed and predicted values was stronger for 2013.  
366 Accuracy decreased at the end of the snow season, when the snowpack was mostly patchy  
367 across the basin; this was particularly the case for the end of the 2012 season. Overall, the  
368 performance of the MLRs was more variable than that of the BRTs, which were more  
369 constant amongst the various snow surveys. For those days on which the models were most  
370 accurate in predicting SD variability, the MLRs showed slightly better scores than the BRTs.  
371 However, for days on which the accuracy between predictions and observations was lower,  
372 the BRTs provided better estimates than the MLRs. For 2012, slightly better results were  
373 obtained using MLRs, while the opposite occurred in 2013. Nevertheless, only large  
374 differences in the accuracy of each model were evident by the end of 2012 snow season, in  
375 the two last surveys, which were characterized by thin and patchy snowpack. In general, there  
376 was good agreement between the models for each survey day, so results obtained with each  
377 model could be compared.

378 As shown for single correlations, the *TPI* variable explained most of the variance in MLR  
379 models developed for all analyzed days (Table 4). The contribution of the other variables

380 varied markedly among surveys, particularly when the two years were compared. In most  
381 cases, *Elevation* was the second most important variable explaining the SD distribution in  
382 2012, followed by *Sx* and *Slope*. The other variables made a much smaller contribution, or  
383 were not included in the models. The contribution of *Elevation* was much less in 2013, and it  
384 was not included in three of the six surveys, whereas in 2012 it was included in all surveys.  
385 For the entire 2013, *Sx* was the second most important variable, followed by *Easting*, which  
386 had an almost negligible influence in 2012. *Northing* was only included in the models for the  
387 surveys carried out during periods dominated by snow accumulation, and was not included in  
388 the models during the periods dominated by melting.

389 Figure 6 shows two examples of BRTs, obtained for the days 2 May 2012 (upper panel) and 3  
390 April 2013 (bottom panel), which accounted for the largest amount of snow accumulation in  
391 each of the two years. The variable *TPI* determined the first branching point, and this  
392 occurred in the majority of the trees obtained (not shown). After the first branching, other  
393 variables were significant in the model, including *Sx* and *TPI* for 2 May 2012, and *Sx* and  
394 *Northing* for 3 April 2013, demonstrating the importance of these variables in the subsequent  
395 branching of the trees.

396 The relative importance (scaled from 0 to 100) of each topographic variable in each BRT is  
397 shown in Table 5. This shows that *TPI* was the first most important variable explaining SD  
398 for all survey days. For the 2012 snow season, *TPI* explained more than 67% of the total  
399 explained variance in all BRTs, and 75% during the accumulation period (the first three  
400 surveys). Thus, for most of the survey days the variance explained by the other variables was  
401 <30%. The second most important variable explaining the SD distribution in 2012 differed  
402 amongst the survey days. Thus, *Sx* was the second most influential variable during May  
403 (except for 24 May 2012), following the largest snowfall in the season (which occurred the 1  
404 May 2012), and *Elevation* was the most important variable in the other surveys during 2012.  
405 *Northing* also had an evident influence during the two first surveys of the year, but

406 subsequently had minimal explanatory capacity, as was the case for all the other variables. In  
407 2013 *TPI* was also the main contributor to the total explained variance, exceeding 50% for  
408 almost all survey days, and approaching or > 70% during the snowmelt period. The influence  
409 of *Sx* was more important in 2013 than in the previous year. At the beginning of 2013 the  
410 contribution of *Sx* to the total explained variance was almost 46%, and remained >20% for the  
411 rest of the snow season; an exception was the last survey, when melting dominated and its  
412 effect declined to 12%. When snow was not mobilized for long periods by wind, the SD  
413 distribution was more dependent on variables related to terrain curvature (*TPI* and  
414 *Curvature*). During 2013, *Elevation* contributed approximately 5% to the total explained  
415 variance during the entire snow season. *Northing* made a significant contribution to the model  
416 (14.7%) on only one day (3 April 2013), and a much smaller contribution on the following  
417 survey day (25 April 2013). Where included in the BRTs, the other variables (*Easting*,  
418 *Radiation*) made no, or only minor, contributions to the total explained variance.

## 419 **5. Discussion**

420 The distribution of snow in mountain areas is highly variable in space and time, as was shown  
421 for the Izas experimental catchment during two consecutive years. Many meteorological and  
422 topographic parameters affect the snow distribution and its evolution through time with  
423 different weights subjected to several factors. In this context, we demonstrated that  
424 topography was a major controlling factor affecting SD in a subalpine catchment, and showed  
425 that its effect evolved during the snow accumulation and melting periods over two years  
426 having highly contrasting climatic conditions and levels of snow accumulation.

427 There have been many studies analyzing the spatial distribution of SD in mountain areas  
428 (Anderton et al., 2004; Erickson et al., 2005; López-Moreno et al., 2010; McCreight et al.,  
429 2012). Besides some researches have also focused their attention in long-term inter-annual  
430 snow distribution analyses (Jepsen et al., 2012; Sturm and Wagner, 2010, Winstral and  
431 Marks, 2014) but there are very few datasets that have enabled investigation of the intra- and

432 inter-annual variability of the topographic control on the snowpack distribution, being  
433 important to investigate both time scales. The results of previous research have highlighted  
434 the difficulties in fully explaining the distribution of snow in complex mountainous terrain. In  
435 addition, the results have differed among studies, and suggest that different variables govern  
436 the distribution of snowpack among areas as consequence of their differing characteristics and  
437 geographical settings, including surface area and altitudinal gradients, the importance of wind  
438 redistribution, the presence or absence of vegetation, and the topographic complexity  
439 (Grünewald et al., 2013).

440 Most of the topographic variables investigated in this study have been included in previous  
441 studies, including *Elevation*, *Slope*, *Radiation*, *Curvature* and *Sx*. Other variables, in  
442 particular *TPI*, have received little attention in previous research (López-Moreno et al., 2010).  
443 We showed that *TPI* at a scale of 25 m had the greatest capacity to explain the SD distribution  
444 in the study catchment. *Curvature* (which refers to a small spatial scale of terrain curvature)  
445 was also highly correlated with the SD distribution, but not as highly as *TPI*, reinforcing the  
446 importance of considering terrain curvature at various scales in explaining the SD distribution  
447 in mountain environments. The correlation between snowpack and the *TPI* decreased during  
448 melting periods, whereas the correlation with *Curvature* remained constant. This suggests that  
449 snow accumulates more in small, deep concavities, but is shallower at the end of the season in  
450 wider concave areas that were identified by the 25 m *TPI* scale. This effect was evident at the  
451 end of the snow season, when snow was present only in deep concavities, as shown in Figure  
452 3. To explain the snow distribution, Anderton et al. (2004) compared the relative elevation of  
453 a cell with the terrain over a 40 m radius, and observed that this had a major role on SD  
454 distribution, what reinforces curvature importance at different scales.

455 The maximum upwind slope (*Sx*; Winstral et al., 2002) has also been identified as a key  
456 variable explaining snow distribution, improving the results obtained when it is introduced  
457 into models. Our results are comparable with those of other studies that have shown that the

458 optimum searching distance for correlating  $S_x$  with the SD distribution is 300 m (Schirmer et  
459 al., 2011), so it is not a large difference for the considered distances in this work which  
460 reaches 500m. As it is observed from the reported wind information, Izas experimental  
461 catchment has W-NW dominant wind direction what is consistent with the best correlated  $S_x$   
462 directions. For this reason, the  $S_x$  preferred direction for each date was selected, and showed  
463 that there were intra-annual shifts in the most highly correlated direction. The change in the  
464 most important  $S_x$  direction was similar between the 2012 and 2013 snow seasons; it started  
465 with a northerly component and evolved to a dominant westerly direction. We also found a  
466 decrease in the correlation between  $S_x$  and the snow distribution at the end of each snow  
467 season, when melting conditions dominated; this is consistent with the findings of previous  
468 studies (Winstral and Marks, 2002).

469  $S_x$  parameter takes into account sheltering effects with topographic origin in relation to wind  
470 directions. As it has been observed in this study, higher SD amounts are observed in leeward  
471 slopes, which for this study site are in E-SE slopes, being perceived this effect in the SD  
472 distribution maps.  $TPI$  is not able to explain snow drifts, because this index considers the  
473 topographic characteristics in all directions. Nevertheless, terrain characteristics at the study  
474 site in relation to SD distribution have shown a higher importance of  $TPI$  when compared to  
475  $S_x$ . The most likely explanation of this result is that the basin has a rather reduced size, shows  
476 the same general aspect (SE facing) and topography is relatively gentle. Under such  
477 conditions, during wind blowing events snow is accumulated in all the wide concavities of the  
478 basin (represented by  $TPI$ ) independently of its specific location. Nonetheless, wind  
479 redistribution will be affected by a combination of local topography in relation to the main  
480 wind directions; what makes necessary to consider the  $S_x$  parameter, and this effect lasts in  
481 time until the melting season is advanced. Nonetheless, under such conditions more snow is  
482 accumulated according to main wind directions; what makes necessary to consider  $S_x$   
483 parameter, and this effect lasts in time until the melting season is advanced.

484 Only for two days (22 February 2012 and 2 April 2012) was there no (or a minor)  
485 contribution of *Sx* to SD, according to the BRTs and MLRs. On these days *Nothing* was  
486 introduced into the models, and was found to explain some of the variance of *Sx* from  
487 northerly direction (the best correlated direction for these days (Table 2).

488 Although *Elevation* has been found to largely explain the snow distribution in areas having  
489 marked altitudinal differences (Elder et al., 1998; Erxleben et al., 2002; Molotch and Bales,  
490 2005) in our study no strong association was found between SD and *Elevation*, with  
491 significant correlations occurring only during the snowmelt period. This is because of the low  
492 elevation range of the study area (300 m). During the accumulation period the entire  
493 catchment is generally above the freezing height. However, during spring the 0°C isotherm  
494 shifts to higher elevations, which may lead to different melting rates within the basin. Despite  
495 the relatively weak correlation between Elevation and SD, this variable was introduced as a  
496 predictor in the MLRs and BRTs for most of the days analyzed. Similarly, López-Moreno et  
497 al. (2010) reported that elevation was of increasing importance as the grid size increased.  
498 Anderton et al. (2004) also informed about the importance of elevation to explain snowpack  
499 distribution in the same study area. The results of the present study suggest the increase in  
500 importance of Elevation at the end of the snow season, and particularly when it is considered  
501 in combination with other topographic variables in MLR and BRT models.

502 *Slope* was only a weak explanatory factor for snow distribution, probably because the slope in  
503 most of the catchment is not sufficient to trigger gravitational movements including  
504 avalanches and slushes during the snowmelt period, which could thin the snowpack on the  
505 steepest slopes (Elder et al., 1998). Maybe some of *Slope* explanatory capacity is included on  
506 *Radiation* explanatory capacity, because it affects solar light incident angle, and also, the  
507 steeper areas of the catchment are in south facing zones, nevertheless quantifying such kind of  
508 effects is highly difficult due to the high complexity of SD dynamic in mountain terrain.

509 *Radiation*, *Northing* and *Easting* showed no close correlation with the snowpack distribution;  
510 their relationships with SD were variable over time, with statistically significant correlations  
511 occurring on some days and only weak correlations on other days. The results suggested that  
512 *Radiation* and *Northing* (which showed almost opposite patterns) may be related to SD for  
513 two different reasons. During the accumulation period in 2013 heavy snowfalls associated  
514 with northerly winds led to the accumulation of deep snow on south-facing (more irradiated)  
515 surfaces, whereas during the snowmelt period the greater exposure of the southern slopes to  
516 solar energy led to a positive (negative) correlation with *Northing* (*Radiation*). This  
517 phenomenon was also observed by López-Moreno et al. (2013), using a physically-based  
518 snow energy balance model in the same study area. Moreover, the high and opposite  
519 correlation between *Northing* and *Radiation* obtained in PCA results (not shown in the  
520 manuscript), prevented us of potential problems of multicollinearity. Thus, only *Northing* was  
521 considered for MLRs and BRTs (the same occurred with *TPI* and *Curvature*, being only  
522 considered in statistical models the *TPI*). Although *Northing* did not show a significant  
523 correlation with SD during accumulation periods, when the surveys were closer to the  
524 snowmelt period the negative correlation of this variable with SD was much more evident,  
525 possibly due to the increase of the difference in the energetic exchange between the sun  
526 exposed and shaded areas. The importance of *Northing* in MLR models, combined with the  
527 contribution of *Easting* during the accumulation period may be related to the high snow  
528 redistribution originated by wind directions from N- NW directions. In such a way terrain  
529 aspect (considered with *Northing* and *Easting*) during winter is more related to the  
530 accumulation patterns resulting from wind redistribution, whereas in spring they were  
531 associated with the unequal distribution of solar radiation, which leads to higher melting rates  
532 on the most irradiated slopes, what has shown better explanatory capacity than *Radiation* at  
533 Izas Experimental catchment.

534 The MLRs and BRTs provided reasonably high accuracy scores when observed and predicted  
535 SD data were compared. The scores were comparable, and in some cases better, to values  
536 reported in previous researches using similar methods. Molotch et al., (2005) reported  $r^2$   
537 values between 0.31 and 0.39 with BRT; and Winstral et al., (2002), considering different  
538 number of terminal nodes of BRT with similar topographic variables, obtained an optimal tree  
539 size of 16 nodes (which is quite similar to the tree size selected in this study, in spite of  
540 differences in the study area, the nature of the dataset, etc) with an  $r^2$  value close to 0.4.  
541 Moreover results presented here were obtained from a separate dataset, and data used to create  
542 the models are not considered for testing, thanks to the large available data set. One reason for  
543 the improvement may be the use of the *TPI* as a SD predictor, as this variable has not been  
544 considered in previous studies. Nevertheless, it should be noted that the study sites considered  
545 in other studies, could differ in terms on complexity of terrain, and also in SD accumulation  
546 amounts. For the 12 survey days the *TPI* had the greatest explanatory capacity in both  
547 approaches. However, based on comparison of the different dates and surveys, the other  
548 variables made more varying contributions, as a result of the different roles they play during  
549 the snow accumulation and melting periods, and the wind conditions during the main snowfall  
550 events. The models had less capacity to explain spatial variability of the snowpack when the  
551 snow was thinner and patchy. The BRT and MLR approaches were consistent with respect to  
552 error estimates. The results obtained using each approach were comparable, so the trends in  
553 the variable ranking for both models for each survey day were very similar. Only during  
554 conditions of snow scarcity did the BRT approach demonstrate better capability to relate SD  
555 to topography. This is probably a consequence of the greater capacity of BRTs to take account  
556 of the nonlinear response of the snowpack to topography, and the occurrence of sharp  
557 thresholds typical of days when the snowpack is patchy (López-Moreno et al., 2010; Molotch  
558 et al., 2005).

559 In spite of model results differ between survey days and years, some variables are always  
560 present in the models and their contribution to the total explained variances are rather similar.  
561 Moreover for 2012 and 2013 a consistent inter-annual distribution of the snow pack in the  
562 catchment is observed; the areas of maximum SD and the location of snow free zones were  
563 consistent between both years of the study, and more importantly there is a strong consistency  
564 of the effect of topography on SD is clear. This spatial consistency of snowpack has  
565 implications for soil dynamics and plant cycles, because some parts of the basin will tend to  
566 remain free of snow cover during longer periods favoring the presence of temporary frozen  
567 soils, and reducing the isolation effect of snowpack to the plants (Keller et al., 2000; Pomeroy  
568 and Gray, 1995). Moreover, it suggests that the information acquired from TLS during several  
569 years could be useful to design long-term monitoring strategies of SD in the basin based on  
570 few manual measurements in representative points according their terrain characteristics.

## 571 **6. Conclusions**

572 Topographic variables related to terrain curvature were shown to contribute more to  
573 explaining snow distribution than other variables. In particular, the *TPI* at a 25 m searching  
574 distance was the major variable explaining SD in the Izas experimental catchment. This  
575 suggests the importance of including this index in future snow studies, and the need to  
576 establish the best searching distance for relating this variable to SD distribution at other study  
577 sites. The maximum upwind slope at a searching distance of 200 m was also an important  
578 variable explaining the SD distribution. However, its influence varied markedly between  
579 years and surveys, depending of the specific wind conditions during the main snowfall events.  
580 The influence of the other topographical variables on the spatial distribution of SD was less,  
581 and showed greater intra- and inter-annual variability. The results from BRTs and MLRs  
582 models were consistent, and the explanatory capacities of the main variables were very  
583 similar for all surveys. This suggests that the effect of topography on snow distribution has  
584 relatively high intra- and inter-annual consistency in the study catchment. Terrain

585 characteristics have shown a major role on snow distribution, as *TPI* explanatory capacity.  
586 When snow distribution could be affected by wind action (mainly during the accumulation  
587 period), its distribution is modified tightly related with main wind directions and sheltering  
588 effects, well described with *Sx* parameter. Several interesting temporal evolutions during the  
589 two snow seasons were found in the relation of some topographic variables to SD.

## 590 **7. Acknowledgments**

591 This study was supported by the research project Hidrología nival en el Pirineo Central  
592 Español: Variabilidad espacial, importancia hidrológica y respuesta a la variabilidad y cambio  
593 climático (CGL2011-27536/HID, Hidronieve) “ CGL2011-27574-CO2-02 and CGL2011-  
594 27536, financed by the Spanish Commission of Science and Technology and FEDER; LIFE  
595 MEDACC, financed by the LIFE programme of the European Commission; “El glaciar de  
596 Monte Perdido: Monitorización y estudio de su dinámica actual y procesos criosféricos  
597 asociados como indicadores de procesos de cambio global844/2013, financed by MAGRAMA  
598 National Parks and CTPP1/12 “Creación de un modelo de alta resolución espacial para  
599 cuantificar la esquiabilidad y la afluencia turística en el Pirineo bajo distintos escenarios de  
600 cambio climático”, financed by the Comunidad de Trabajo de los Pirineos. The first author is  
601 a recipient under the pre-doctoral FPU grant program 2010 (Spanish Ministry of Education  
602 Culture and Sports). The third author was the recipient of the postdoctoral grants JAE-  
603 DOC043 (CSIC) and JCI-2011-10263 (Spanish Ministry of Science and Innovation). The  
604 authors thank Adam Winstral for the use of his algorithm for calculating maximum upwind  
605 slope.

## 606 **8. References**

607 Anderton, S.P., White, S.M., and Alvera, B.: Evaluation of spatial variability in snow water  
608 equivalent for a high mountain catchment. *Hydrol. Process.*, 18, 435–453, 2004.

609 Bales, R.C., and Harrington, R.F.: Recent progress in snow hydrology. *Reviews of*  
610 *Geophysics Supplement*, 33, 1011–1020, 1995.

611 Barnett, T.P., Adam, J.C., and Lettenmaier, D.P.: Potential impacts of a warming climate on  
612 water availability in snow-dominated regions. *Nature*, 438, 303–309, 2005.

613 Del Barrio, G., Alvera, B., Puigdefabregas, J., and Diez, C.: Response of high mountain  
614 landscape to topographic variables: Central pyrenees. *Landscape Ecol.*, 12, 95–115, 1997.

615 Beale, C.M., Lennon, J.J., Yearsley, J.M., Brewer, M.J., and Elston, D.A.: Regression  
616 analysis of spatial data. *Ecol. Lett.*, 13, 246–264, 2010.

617 Beniston, M.: Climatic Change in Mountain Regions: A Review of Possible Impacts. *Climatic*  
618 *Change*, 59, 5–31, 2003.

619 Breiman, L.: *Classification and regression trees* (Wadsworth International Group). 1984.

620 Caballero, Y., Voirin-Morel, S., Habets, F., Noilhan, J., LeMoigne, P., Lehenaff, A., and  
621 Boone, A.: Hydrological sensitivity of the Adour-Garonne river basin to climate change.  
622 *Water Resour., Res.* 43, W07448, 2007.

623 Deems, J.S., Fassnacht, S.R., and Elder, K.J.: Fractal Distribution of Snow Depth from Lidar  
624 Data. *J. Hydrometeorol.*, 7, 285–297, 2006

625 De Rue, J., Bourgeois, J., Bats, M., Zwertvaegher, A., Gelorini, V., De Smedt., P.M., Chu,  
626 W., Antrop., M., De Maeyer, P., Finke., P., Mairvanne, M.V., Verniers., J. and Crombé., P.:  
627 Application of the topographic position index to heterogeneous landscapes. *Geomorphology*.  
628 186 , 39-49. 2013.

629 Deems, J.S., Fassnacht, S.R., and Elder, K.J.: Interannual Consistency in Fractal Snow Depth  
630 Patterns at Two Colorado Mountain Sites. *J. Hydrometeorol.* 9, 977–988, 2008

631 Egli, L., Jonas, T., Grünewald, T., Schirmer, M., and Burlando, P.: Dynamics of snow  
632 ablation in a small Alpine catchment observed by repeated terrestrial laser scans. *Hydrol.*  
633 *Process.*, 26, 1574–1585. 2012.

634 Elder, K., Dozier, J., and Michaelsen, J.: Snow accumulation and distribution in an Alpine  
635 Watershed. *Water Resour. Res.*, 27, 1541–1552, 1991.

636 Elder, K., Rosenthal, W., and Davis, R.E.: Estimating the spatial distribution of snow water  
637 equivalence in a montane watershed. *Hydrol. Process.* 12, 1793–1808, 1998.

638 Elsner, J.B., and Schmertmann, C.P. (1994). Assessing Forecast Skill through Cross  
639 Validation. *Wea. Forecasting* 9, 619–624.

640 Erickson, T.A., Williams, M.W., and Winstral, A.: Persistence of topographic controls on the  
641 spatial distribution of snow in rugged mountain terrain, Colorado, United States. *Water*  
642 *Resour. Res.*, 41 (4), 1–17, 2005.

643 Erxleben, J., Elder, K., and Davis, R.: Comparison of spatial interpolation methods for  
644 estimating snow distribution in the Colorado Rocky Mountains. *Hydrol. Process.*, 16, 3627–  
645 3649, 2002.

646 Fassnacht, S.R., and Deems, J.S.: Measurement sampling and scaling for deep montane snow  
647 depth data. *Hydrol. Process.*, 20, 829–838, 2006.

648 Fassnacht, S.R., Dressler, K.A., and Bales, R.C.: Snow water equivalent interpolation for the  
649 Colorado River Basin from snow telemetry (SNOTEL) data. *Water Resour. Res.*, 39 (8),  
650 SWC31–SWC310, 2003.

651 Fassnacht, S.R., López-Moreno, J.I., Toro, M., and Hultstrand, D.M.: Mapping snow cover  
652 and snow depth across the Lake Limnopolar watershed on Byers Peninsula, Livingston Island,  
653 Maritime Antarctica. *Antarct. Sci.*, 25, 157–166, 2013.

654 Fu, P., and Rich, P.M.: A geometric solar radiation model with applications in agriculture and  
655 forestry. *Computers and Electronics in Agriculture*, 37, 25–35, 2002.

656 Groffman, P.M., Driscoll, C.T., Fahey, T.J., Hardy, J.P., Fitzhugh, R.D., and Tierney, G.L.:  
657 Colder soils in a warmer world: A snow manipulation study in a northern hardwood forest  
658 ecosystem. *Biogeochemistry*, 56, 135–150, 2001.

659 Grünewald, T., Schirmer, M., Mott, R., and Lehning, M. Spatial and temporal variability of  
660 snow depth and ablation rates in a small mountain catchment. *The Cryosphere*, 4, 215–225,  
661 2010.

662 Grünewald, T., Stötter, J., Pomeroy, J.W., Dadic, R., Moreno Baños, I., Marturià, J., Spross,  
663 M., Hopkinson, C., Burlando, P., and Lehning, M.: Statistical modelling of the snow depth  
664 distribution in open alpine terrain. *Hydrol. Earth Syst. Sci.*, 17, 3005–3021. 2013

665 Hosang, J., and Dettwiler, K.: Evaluation of a water equivalent of snow cover map in a small  
666 catchment area using a geostatistical approach. *Hydrol. Process.*, 5, 283–290., 1991.

667 Jepsen, S.M., Molotch, N.P., Williams, M.W., Rittger, K.E., and Sickman, J.O. (2012).  
668 Interannual variability of snowmelt in the Sierra Nevada and Rocky Mountains, United  
669 States: Examples from two alpine watersheds. *Water Resour. Res.* 48, W02529.

670 Jost, G., Weiler, M., Gluns, D.R., and Alila, Y.: The influence of forest and topography on  
671 snow accumulation and melt at the watershed-scale. *Journal of Hydrology*, 347, 101–115,  
672 2007.

673 Keller, F., Kienast, F., and Beniston, M.: Evidence of response of vegetation to environmental  
674 change on high-elevation sites in the Swiss Alps. *Reg. Environ. Change*, 1, 70–77, 2002.

675 Lehning, M., Löwe, H., Ryser, M., and Raderschall, N.: Inhomogeneous precipitation  
676 distribution and snow transport in steep terrain. *Water Resour. Res.*, 44, W07404, 2008.

677 Lehning, M., Grünewald, T., and Schirmer, M. (2011). Mountain snow distribution governed  
678 by an altitudinal gradient and terrain roughness. *Geophysical Research Letters* 38.

679 Liston, G.E.: Interrelationships among Snow Distribution, Snowmelt, and Snow Cover  
680 Depletion: Implications for Atmospheric, Hydrologic, and Ecologic Modeling. *J. Appl.*  
681 *Meteorol.*, 38, 1474–1487, 1999.

682 López-Moreno, J.I., and Nogués-Bravo, D.: A generalized additive model for the spatial  
683 distribution of snowpack in the Spanish Pyrenees. *Hydrol. Process.*, 19, 3167–3176, 2005.

684 López-Moreno, J.I., Latron, J., and Lehmann, A.: Effects of sample and grid size on the  
685 accuracy and stability of regression-based snow interpolation methods. *Hydrol. Process.*, 24,  
686 1914–1928, 2010.

687 López-Moreno, J.I., Vicente-Serrano, S.M., Morán-Tejeda, E., Lorenzo-Lacruz, J., Kenawy,  
688 A., and Beniston, M.: Effects of the North Atlantic Oscillation (NAO) on combined  
689 temperature and precipitation winter modes in the Mediterranean mountains: Observed  
690 relationships and projections for the 21st century. *Global Planet. Change*, 77, 62–76, 2011.

691 López-Moreno, J.I., Fassnacht, S.R., Heath, J.T., Musselman, K.N., Revuelto, J., Latron, J.,  
692 Morán-Tejeda, E., and Jonas, T.: Small scale spatial variability of snow density and depth  
693 over complex alpine terrain: Implications for estimating snow water equivalent. *Adv. Water*  
694 *Resour.*, 55, 40–52, 2012a.

695 López-Moreno, J.I., Pomeroy, J.W., Revuelto, J., and Vicente-Serrano, S.M.: Response of  
696 snow processes to climate change: spatial variability in a small basin in the Spanish Pyrenees.  
697 *Hydrol. Process.*, 27, 2637–2650, 2012b.

698 McCreight, J.L., Slater, A.G., Marshall, H.P., and Rajagopalan, B.: Inference and uncertainty  
699 of snow depth spatial distribution at the kilometre scale in the Colorado Rocky Mountains:  
700 The effects of sample size, random sampling, predictor quality, and validation procedures.  
701 *Hydrol. Process.*, 28, 933–957. 2014.

702 Molotch, N.P., and Bales, R.C.: Scaling snow observations from the point to the grid element:  
703 Implications for observation network design. *Water Resour. Res.*, 41, W11421, 2005.

704 Molotch, N.P., Colee, M.T., Bales, R.C., and Dozier, J.: Estimating the spatial distribution of  
705 snow water equivalent in an alpine basin using binary regression tree models: the impact of  
706 digital elevation data and independent variable selection. *Hydrol. Process.*, 19, 1459–1479,  
707 2005.

708 Mott, R., Schirmer, M., Bavay, M., Grünwald, T., and Lehning, M.: Understanding snow-  
709 transport processes shaping the mountain snow-cover. *The Cryosphere*, 4, 545–559, 2010.

710 Mott, R., Schirmer, M., and Lehning, M.: Scaling properties of wind and snow depth  
711 distribution in an Alpine catchment. *J. Geophys. Res.-Atmos.*, 116, D06106, 2011.

712 Mott, R., Gromke, C., Grünewald, T., and Lehning, M. (2013). Relative importance of  
713 advective heat transport and boundary layer decoupling in the melt dynamics of a patchy  
714 snow cover. *Advances in Water Resources* 55, 88–97.

715 Pomeroy, J.W., and Gray, D.M.: Snowcover accumulation, relocation, and management.  
716 National Hydrology Research Institute, Saskatoon, Sask., Canada, 1995.

717 Pomeroy, J., Essery, R., and Toth, B.. Implications of spatial distributions of snow mass and  
718 melt rate for snow-cover depletion: observations in a subarctic mountain catchment. *Ann.*  
719 *Glaciol.*, 38, 195–201, 2004.

720 Prokop, A.: Assessing the applicability of terrestrial laser scanning for spatial snow depth  
721 measurements. *Cold Reg. Sci. Technol.*, 54, 155–163, 2008.

722 Prokop, A., Schirmer, M., Rub, M., Lehning, M., and Stocker, M., A comparison of  
723 measurement methods: terrestrial laser scanning, tachymetry and snow probing for the  
724 determination of the spatial snow-depth distribution on slopes. *Ann. Glaciol.*, 49, 210–216,  
725 2008.

726 Revuelto, J., López-Moreno, J.I., Azorin-Molina, C., Zabalza, J., Arguedas, G., and Vicente-  
727 Serrano, S.M.: Mapping the annual evolution of snow depth in a small catchment in the  
728 Pyrenees using the long-range terrestrial laser scanning. *Journal of Maps*, 1–15., DOI:  
729 10.1080/17445647.2013.869268, 2014.

730 Schaffhauser, A., Adams, M., Fromm, R., Jörg, P., Luzi, G., Noferini, L., and Sailer, R.:  
731 Remote sensing based retrieval of snow cover properties. *Cold Reg. Sci. Technol.*, 54, 164–  
732 175, 2008.

733 Schirmer, M., and Lehning, M.: Persistence in intra-annual snow depth distribution: 2. Fractal  
734 analysis of snow depth development. *Water Resour. Res.*, 47, W09517, 2011.

735 Schirmer, M., Wirz, V., Clifton, A., and Lehning, M.: Persistence in intra-annual snow depth  
736 distribution: 1. Measurements and topographic control. *Water Resour. Res.*, 47, W09516,  
737 2011.

738 Scipión, D.E., Mott, R., Lehning, M., Schneebeli, M., and Berne, A.: Seasonal small-scale  
739 spatial variability in alpine snowfall and snow accumulation. *Water Resour. Res.*, 49, 1446–  
740 1457, 2013.

741 Steger, C., Kotlarski, S., Jonas, T., and Schär, C.: Alpine snow cover in a changing climate: a  
742 regional climate model perspective. *Clim. Dynam.*, 1–20, 2012.

743 Sturm, M., and Wagner, A.M. (2010). Using repeated patterns in snow distribution modeling:  
744 An Arctic example. *Water Resources Research* 46.

745 Trujillo, E., Ramírez, J.A., and Elder, K.J.: Topographic, meteorologic, and canopy controls  
746 on the scaling characteristics of the spatial distribution of snow depth fields. *Water Resour.*  
747 *Res.*, 43, W07409, 2007.

748 Watson, F.G.R., Anderson, T.N., Newman, W.B., Alexander, S.E., and Garrott, R.A.:  
749 Optimal sampling schemes for estimating mean snow water equivalents in stratified  
750 heterogeneous landscapes. *Journal of Hydrology* 328, 432–452, 2006.

751 Weiss, A.D.: Topographic position and landforms analysis. ESRI user conference, San Diego  
752 USA, 2001.

753 Willmott, C.J. On the Validation of Models. *Phys. Geogr.*, 2, 184–194, 1981.

754 Winstral, A., and Marks, D.: Simulating wind fields and snow redistribution using terrain-  
755 based parameters to model snow accumulation and melt over a semi-arid mountain  
756 catchment. *Hydrol. Process.*, 16, 3585–3603, 2002.

757 Winstral, A., Elder, K., and Davis, R.E.: Spatial Snow Modeling of Wind-Redistributed Snow  
758 Using Terrain-Based Parameters. *Journal of Hydrometeorol.*, 3, 524–538, 2002.

759 Winstral, A., and Marks, D. (2014). Long-term snow distribution observations in a mountain  
760 catchment: Assessing variability, time stability, and the representativeness of an index site.  
761 *Water Resour. Res.* 50, 293–305.

762 Wipf, S., Stoeckli, V., and Bebi, P.: Winter climate change in alpine tundra: plant responses  
763 to changes in snow depth and snowmelt timing. *Climatic Change*, 94, 105–121, 2009.

764

765

766

767

768

769

770

771

772

773

774

775

776

777

778

779

780

781

782

783

784

785

786 **9. Tables**

	Snow season 2012						Snow season 2013					
	22/02	02/04	17/04	02/05	14/05	24/05	17/02	03/04	25/04	06/06	12/06	20/06
Mean SD (m)	0.72	0.58	0.60	0.97	0.71	0.70	2.98	3.22	2.53	2.28	2.09	1.61
Max SD (m)	5.5	3.8	5.3	6.1	4.4	4.3	10.9	11.2	10.1	9.6	8.9	7.9
SCA (%)	67.2	33.5	94.1	98.8	30.9	18.9	98.8	100.0	96.3	86.4	77.1	67.0

787

788 **Table 1:** Summary statistics of the snowpack distribution and the snow covered area of the  
 789 basin. Note that snow covered area is expressed as a % of the total area surveyed by the TLS,  
 790 and the mean SD is the average of all SDs not including zero values.

	Snow season 2012						Snow season 2013					
	22/02	02/04	17/04	02/05	14/05	24/05	17/02	03/04	25/04	06/06	12/06	20/06
Sx 0°	0,19	0,13	0,09	-0,11	0,06	-0,01	0,51*	0,40*	0,31*	0,23*	0,22*	0,20*
Sx 45°	0,15	-0,02	0,00	-0,16	-0,08	-0,09	0,36*	0,25*	0,17	0,12	0,12	0,12
Sx 90°	0,12	-0,14	-0,07	0,11	-0,11	-0,03	-0,15	-0,15	-0,10	-0,09	-0,09	-0,10
Sx 135°	0,02	-0,05	0,05	0,26*	0,01	0,11	-0,27*	-0,19	-0,10	-0,06	-0,06	-0,06
Sx 180°	0,02	0,14	0,15	0,38*	0,17	0,21*	-0,19	-0,08	0,02	0,08	0,08	0,12
Sx 225°	0,12	0,29*	0,26*	<b>0,44*</b>	<b>0,32*</b>	<b>0,23*</b>	0,06	0,18	0,26*	0,29*	0,29*	0,31*
Sx 270°	0,20*	<b>0,33*</b>	<b>0,34*</b>	0,26*	0,27*	0,21*	0,48*	<b>0,52*</b>	<b>0,49*</b>	<b>0,45*</b>	<b>0,42*</b>	<b>0,43*</b>
Sx 315°	<b>0,22*</b>	0,26*	0,27*	0,01	0,22*	0,12	<b>0,56*</b>	0,50*	0,41*	0,34*	0,32*	0,33*

791

792 **Table 2:** Pearson’s r coefficients between SD and Sx, calculated for the eight studied wind  
 793 directions over the survey days. \* marks those correlations that were statistically significant  
 794 ( $\alpha < 0.05$ ) in at least the half of the samples (500 out of 1000 samples) from the Monte Carlo  
 795 approach, and bold r coefficients represent the best correlated Sx direction for a specific  
 796 survey day.

797

798

799

	Snow season 2012						Snow season 2013					
	22/02	02/04	17/04	02/05	14/05	24/05	17/02	03/04	25/04	06/06	12/06	20/06
<b>Elev.</b>	0,09	0,26*	0,16	0,10	0,29*	0,19	0,09	0,18	0,13	0,18	0,21*	0,26*
<b>Slope</b>	0,06	0,18	0,02	-0,03	0,20*	0,03	0,25*	0,27*	0,20*	0,20*	0,21*	0,26*
<b>Curv</b>	-0,44*	-0,45*	-0,47*	-0,49*	-0,41*	-0,37*	-0,39*	-0,40*	-0,40*	-0,39*	-0,38*	-0,38*
<b>North</b>	-0,06	0,00	0,04	0,19	0,07	0,11	-0,38*	-0,27*	-0,19	-0,09	-0,06	-0,11
<b>East.</b>	0,09	0,21*	0,13	0,13	0,13	0,11	0,25*	0,26*	0,27*	0,22*	0,18	0,14
<b>Rad</b>	0,05	0,04	-0,06	-0,22*	-0,12	-0,11	0,36*	0,21*	0,10	-0,09	-0,12	-0,23*
<b>TPI 25</b>	<b>-0,56*</b>	<b>-0,46*</b>	<b>-0,54*</b>	<b>-0,58*</b>	<b>-0,40*</b>	<b>-0,32*</b>	<b>-0,66*</b>	<b>-0,68*</b>	<b>-0,68*</b>	<b>-0,66*</b>	<b>-0,63*</b>	<b>-0,61*</b>
<b>Sx</b>	0,22*	0,33*	0,34*	0,44*	0,32*	0,23*	0,56*	0,52*	0,49*	0,45*	0,42*	0,43*

800

801 **Table 3:** Pearson's r coefficients between SD and the topographic variables. \* marks those  
802 correlations that were statistically significant ( $\alpha < 0.05$ ) in at least the half of the samples (500  
803 out of 1000 samples) from the Monte Carlo approach, and bold r coefficients represent the  
804 best correlated topographic variable for a specific survey day.

805

	Snow season 2012						Snow season 2013					
	22/02	02/04	17/04	02/05	14/05	24/05	17/02	03/04	25/04	06/06	12/06	20/06
<b>TPI</b>	-0,69	-0,53	-0,60	-0,59	-0,48	-0,40	-0,78	-0,72	-0,73	-0,80	-0,74	-0,72
<b>Sx</b>		0,11	0,28	0,26	0,20	0,16	0,36	0,31	0,43	0,37	0,38	0,31
<b>Elev.</b>	0,09	0,22	0,34	0,27	0,27	0,35		0,14		0,08		0,13
<b>Slope</b>		-0,25	-0,29	-0,24	-0,21	-0,21		-0,10	-0,14	-0,16	-0,09	-0,15
<b>North</b>	-0,22	0,13	-0,16				-0,12	-0,11	-0,11			
<b>East.</b>	0,10						0,29	0,25	0,25	0,31	0,23	0,20
<b>r2</b>	0,45	0,31	0,40	0,47	0,33	0,25	0,65	0,63	0,60	0,60	0,57	0,51

806

807 **Table 4:** Multiple linear regression beta coefficients for each independent variable and  
808 sampled day.

809

810

811

812

813

814

	Snow season 2012						Snow season 2013					
	22/02	02/04	17/04	02/05	14/05	24/05	17/02	03/04	25/04	06/06	12/06	20/06
<b>TPI</b>	83.2	78.8	75.0	71.7	74.0	66.9	49.1	56.4	64.4	71.2	69.9	77.5
<b>Sx</b>			4.6	12.7	13.4	10.8	45.9	23.1	23.0	21.8	20.1	12.5
<b>Elev.</b>	5.7	6.8	13.2	9.1	8.2	15.2	5.0	5.7	5.0	3.3	5.9	5.4
<b>Slope</b>	1.7	5.4	5.7	6.5	3.2	7.0			2.1			
<b>North</b>	9.3	8.1	1.5		1.3			14.7	4.3	2.4	2.9	3.6
<b>East.</b>									1.2	1.3	1.1	1.0
<b>r2</b>	0.56	0.42	0.52	0.54	0.46	0.39	0.58	0.56	0.55	0.54	0.53	0.51

815

816 **Table 5:** Contribution of the various topographic variables to the explained variance of SD  
817 distribution in the binary regression models for 2012 and 2013. Values have been rescaled  
818 from 0 to 100.

819

820

821

822

823

824

825

826

827

828

829

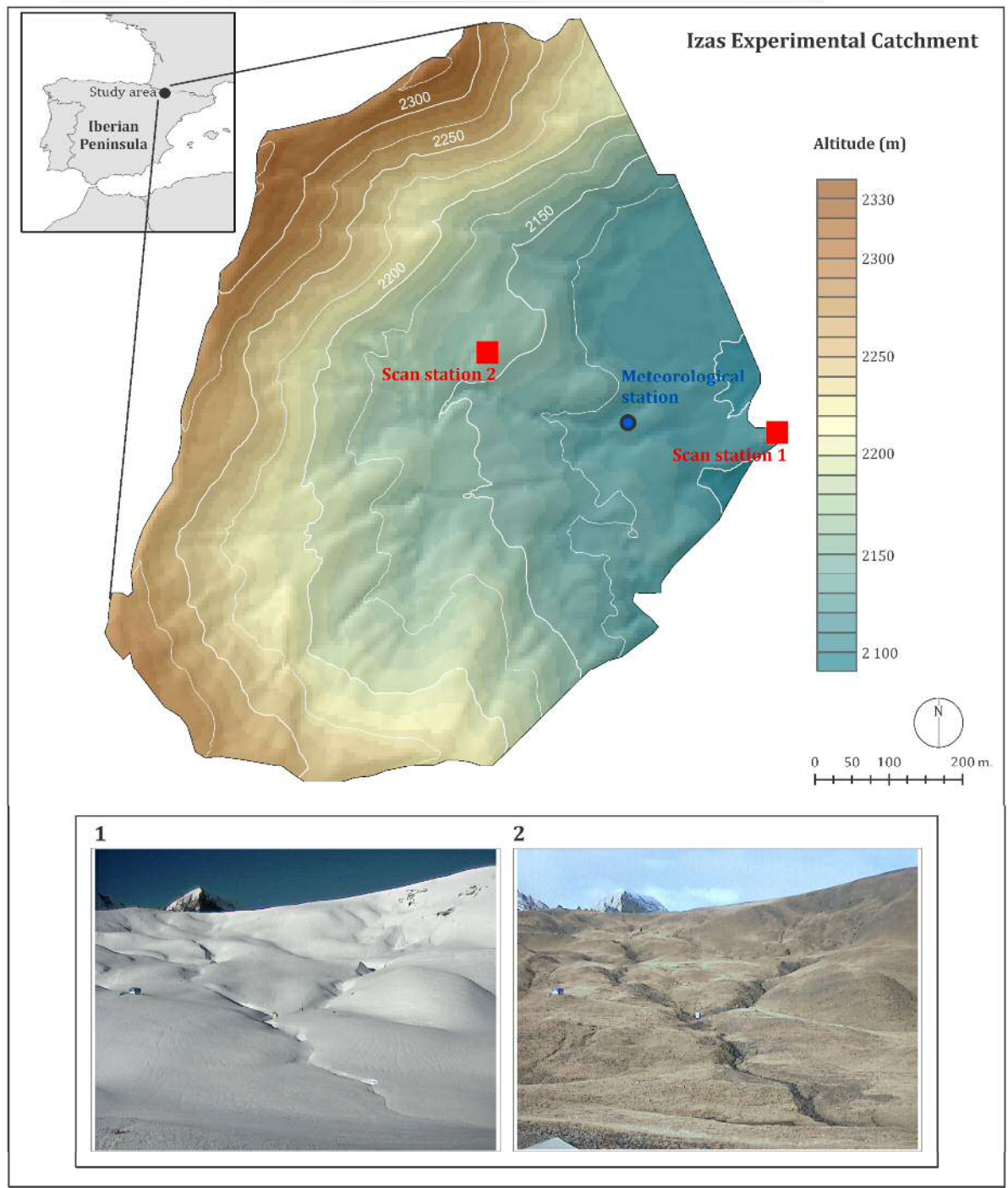
830

831

832

833

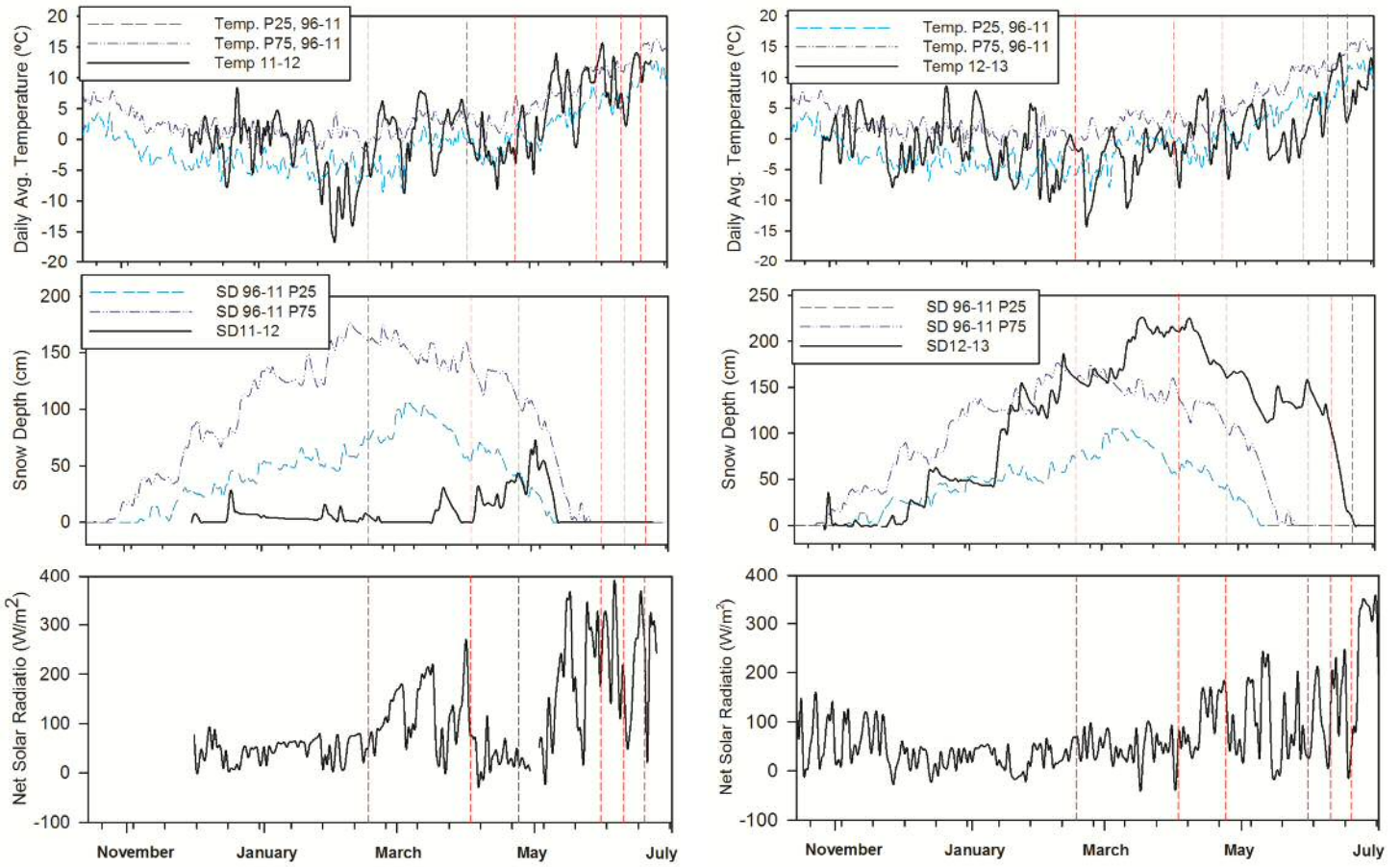
834



836

837 **Figure 1:** Location of the Izas experimental catchment, and the digital elevation model  
838 showing the positions of the scan stations and the automatic meteorological station. The two  
839 images in the bottom part of the figure, from Scan Station 1, show the terrain characteristics  
840 with (1) and without snow cover (2).

841



843

844 **Figure 2:** Daily average temperature, snow depth and net solar radiation at the automatic  
 845 weather station (AWS) for the 2012 (left) and 2013 (right) snow seasons. The continuous  
 846 lines represent the daily values for 2012 and 2013, and the dashed lines show the 25th and  
 847 75th percentiles of historical daily series (1996–2011). The vertical dashed lines show the  
 848 TLS survey days. Note that during some surveys no snow was present at the AWS, but some  
 849 areas of the Izas experimental catchment were covered by snow.

850

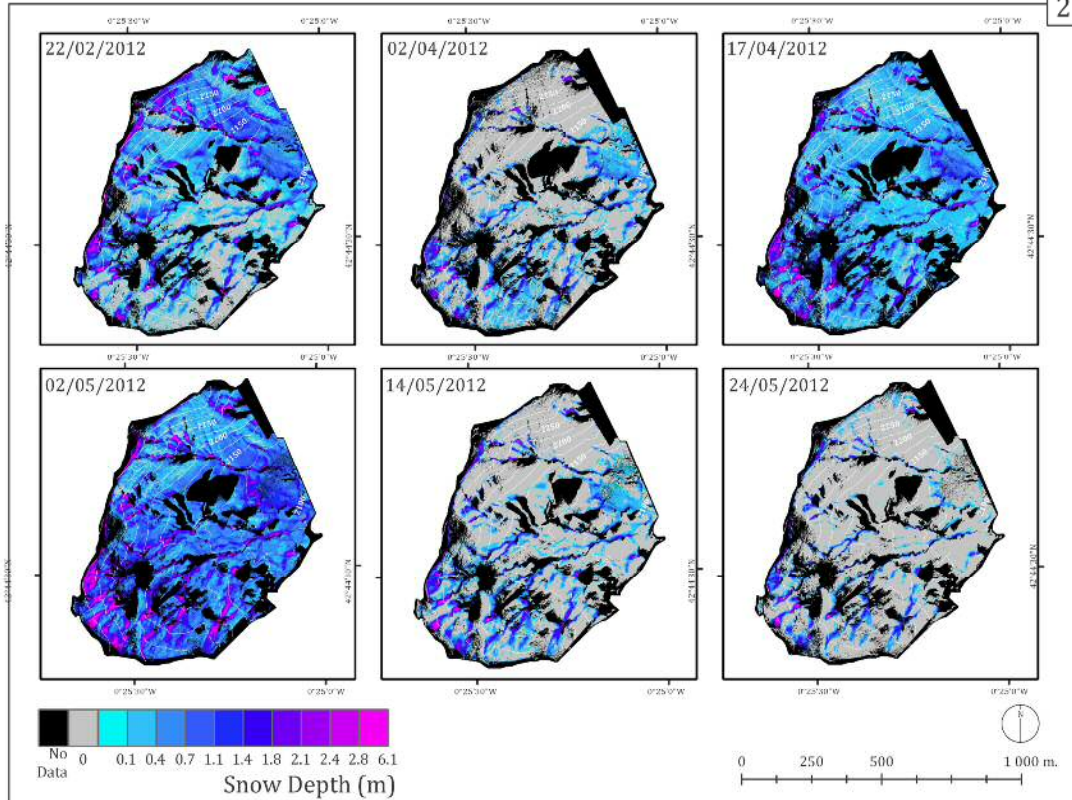
851

852

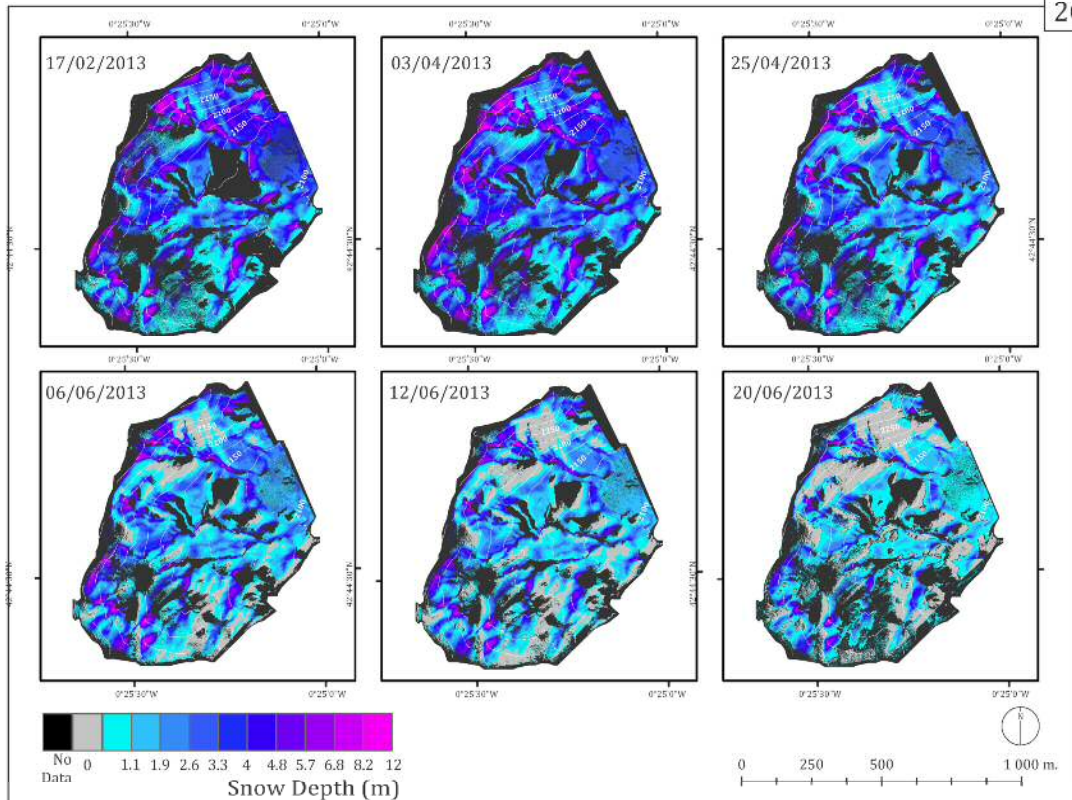
853

## Snow Depth in Izas Experimental Catchment

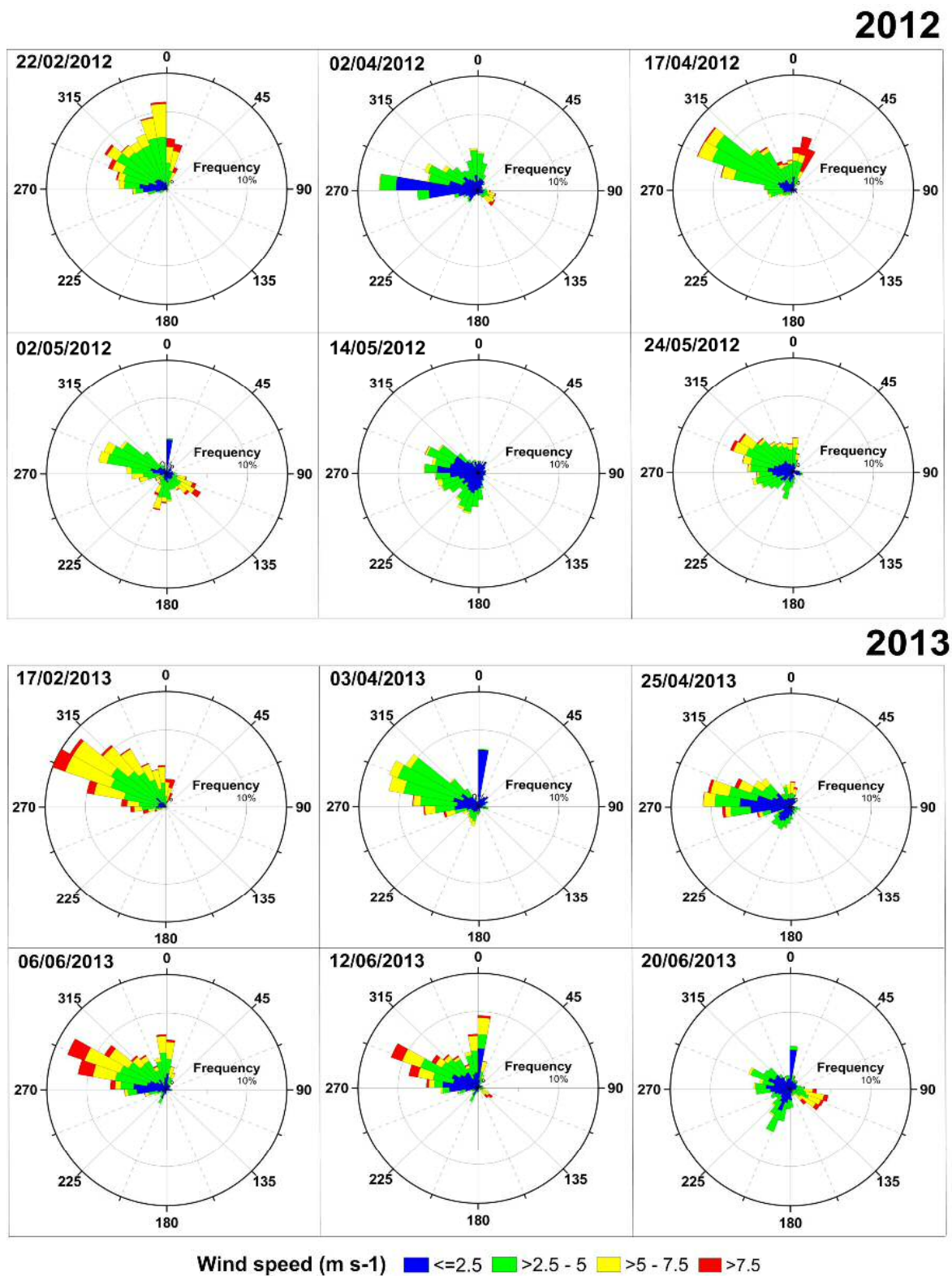
2012



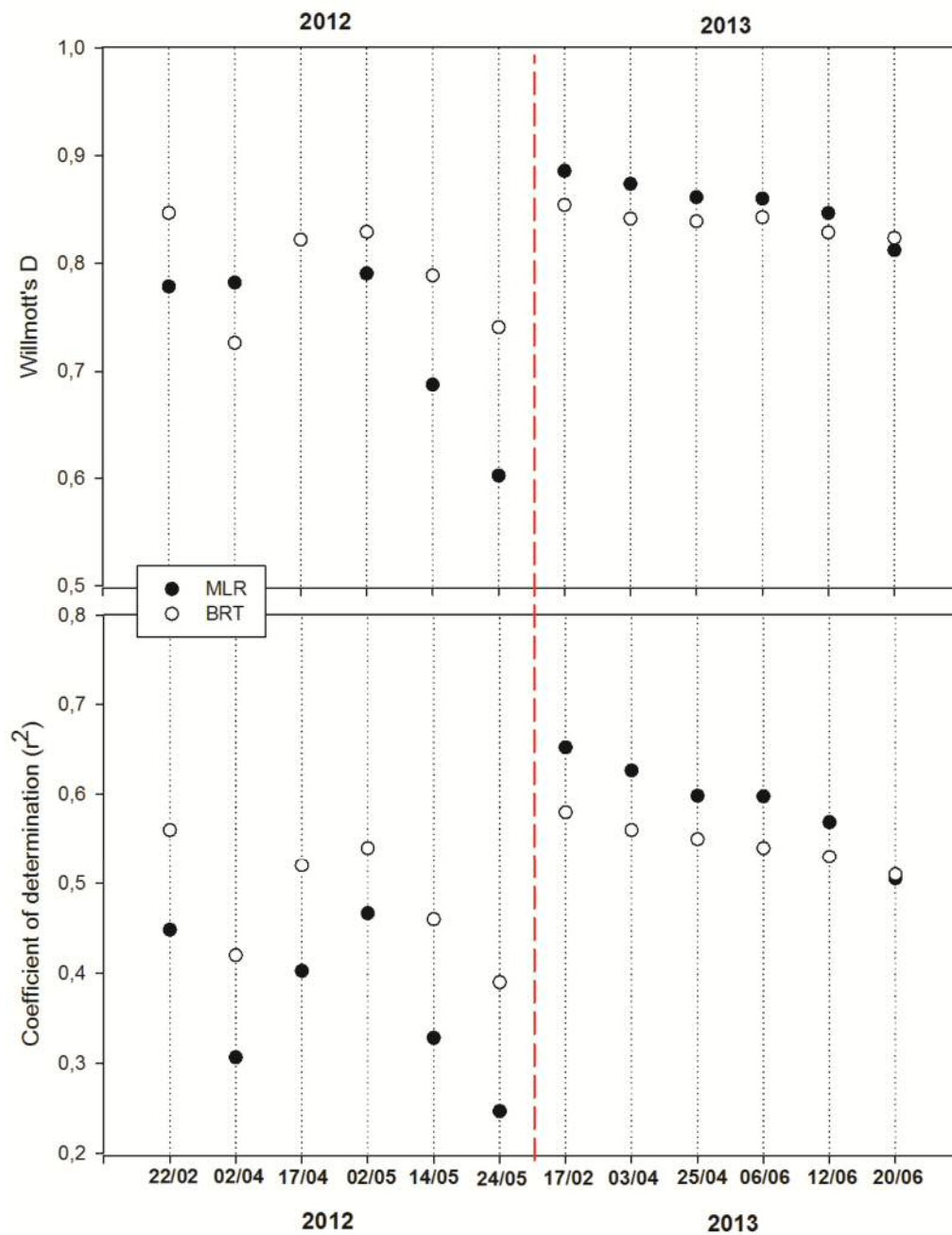
2013



855 **Figure 3:** Spatial distribution of snow depth in the Izas experimental catchment in the surveys  
 856 undertaken in 2012 and 2013.



857  
 858 **Figure 4:** Wind roses from the automatic weather station placed at the catchment obtained for  
 859 a 15 day period.

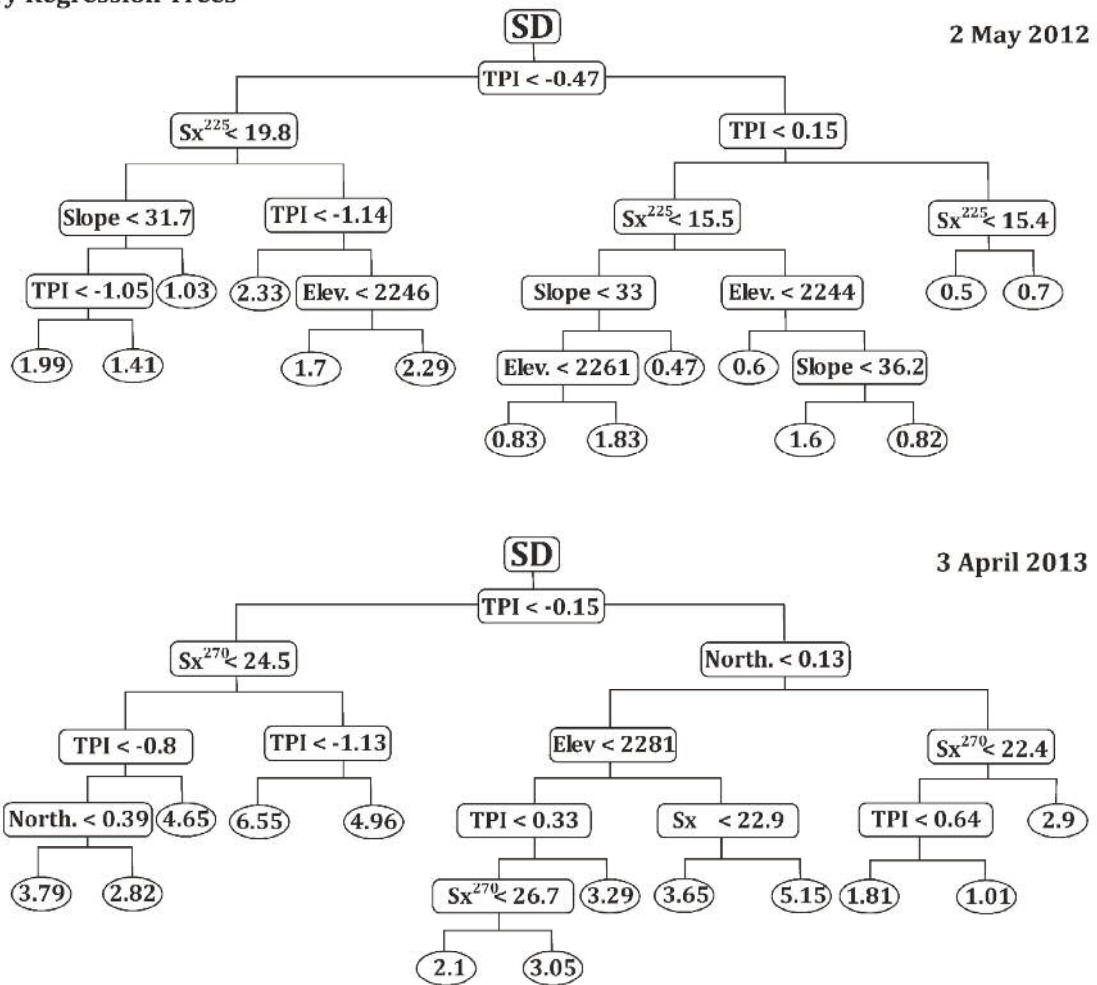


860

861 **Figure 5:** Willmott's D and  $r^2$  values between the observed and predicted SD, based on the  
 862 multiple linear and binary regression models for all survey days.

863

Binary Regression Trees



864

865 **Figure 6:** Binary regression tree obtained for 2 May 2012(top) and 3 April 2013 (bottom).  
 866 The final nodes (with ellipses) show the predicted SD in the zone having the specified terrain  
 867 characteristics. At each branch point, one topographic variable is considered; if the value is  
 868 less than the specified value, the left branch is selected, but if it is equal to or greater than the  
 869 specified value, the right branch is selected.